

We are IntechOpen, the world's leading publisher of Open Access books Built by scientists, for scientists

6,900

Open access books available

186,000

International authors and editors

200M

Downloads

Our authors are among the

154

Countries delivered to

TOP 1%

most cited scientists

12.2%

Contributors from top 500 universities



WEB OF SCIENCE™

Selection of our books indexed in the Book Citation Index
in Web of Science™ Core Collection (BKCI)

Interested in publishing with us?
Contact book.department@intechopen.com

Numbers displayed above are based on latest data collected.
For more information visit www.intechopen.com



Optical Fiber Microsensor of Semidrop

Esteban Molina-Flores, R. B. López-Flores, Daniel Molina-Flores,
 José A. Dávila-Píntle, Germán A. Muñoz-Hernández
 Carlos A. Gracios-Marín and Enrique Morales-Rodríguez
*Benemérita Universidad Autónoma de Puebla, FCE, Optoelectrónica
 México*

1. Introduction

The optical fiber systems until now have turned out to be an ample resource that offers alternatives for tasks of detection and transduction of the energy forms, as a classification of these optical fiber transducers, in this task we presented a sensor that belongs to those of the refractometric type. Since 1995, researchers Khotiaintsev Sergei, Victor De Leon Paredes, Esteban Molina Flores, Alexandre Zemliak made a theoretical modeling analysis of a variety of refractometric sensors based on a pair of fiber optic ends, all useful for measurement of refractive indices. These sensors had an oblique disposition, and these researches are conducted the analysis of best response on the degree of misalignment of two fibers, and to the resulting form of its hemispherical surface of contact with surrounding means. These researches always were within the theoretical regime and for monochromatic irradiation, and never had a tangible evidence of an experimental result (Jones & Zimmer, 1978; Molina-Flores, 1995; Khotiaintsev et al, 1996, 2000, 2002). In 2005 the researcher Esteban Molina Flores, main adviser of this work, proposed and managed to realize the micromachining, one of this microsensorial element with technology of electrical arc, in his particular parallel fiber version, and with surface of semidrop, obtaining theoretical and experimental results in his characterization in the infrared region (1550 nm) for this refractometric microsensor. Like integral part of the research line, the refractometric sensors developed by researcher Esteban Molina Flores (Molina-Flores, 2006), in this occasion through this project, theoretical and experimental results from this microsensor operating in the infrared region are presented, whose particular applying are to solve the problem of the detection, identification and measurement of liquid levels in a cistern tank, by means of the identification of the interface of the immiscible liquids: water and oil engine, and of the interface air-oil engine. The objectives of this work are divided in two kinds of objectives: General objective: realize the characterization of a refractometric microsensor in the infrared region. Particular objectives: a) Make our own sensor of semidrop, b) Establish the conditions of the installation and application of the microsensor with which its efficient operation is guaranteed, c) To realize the theoretical proposal of a design of application of the microsensor of semidrop for the detection of a pair of immiscible liquids. The order in which the sections were considered, obeys to the intention to show the reader the development stages through which it passed the microsensor until the publication of the results in indexed magazine.

2. Manufacturing of the microsensor

In this project the methodology of manufacture of a refractometric microsensor of fiber is presented, which is elaborated from a pair of adjacent fiber tips of parallel disposition, which are fused on a specific form in one of its ends to form a semidrop that serves like detection or refractometric interaction surface with the liquid in submission, see Fig. 1.

2.1 Optical fiber microsensor micromachining

The technology implemented in this project is based on heat source by electrical arc.

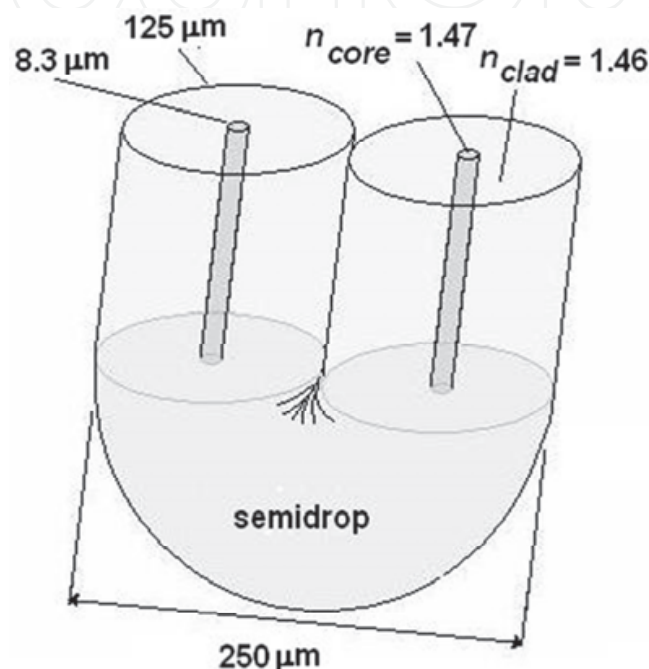


Fig. 1. Disposition of fibers and the fused region is the formed semidrop

The physical manufacture of the microsensor is repeatable every time respecting the characteristics of electric power applied to melt the glass fiber to 1900 ° C, and the specific moments and points in which they are applied time and time again to obtain the form of the semidrop, and to guarantee therefore the awaited optical response in this microsensor. This sensor can be excited with a visible or infrared irradiation source, behaving the fibers like fibers monomodal or multimodal, respectively. The preparation of the optical fiber ends is of the same way in which the optical fiber ends are prepared to realize a common and current splice of low loss. This procedure consists of removing two centimeters of polymer in each fiber end, and realizing an orthogonal cut to the fiber axis, right in its end. After being carefully cleaned with a clean cloth and acetone each of these ends, it can be verified through the camera of the optical fiber splicer machine. Once prepared fibers, they are placed in parallel way, within the fusion chamber of the splicer machine, so that the electrical arc is applied to them, as is shown en Fig. 2.

2.2 Installation of the pair of optical fiber ends in the electrical arc

As experimental installation was used the chamber of fusion of the optical fiber splicer, Fitel mark, whose loss record per splice is of 0,01 dB to monomode fiber, each splice can be realized in a lapse of 13 seconds approximately. The optical fiber splicer is a machine that

radiates electrical arcs whose electric power are of 20 W to splice fiber monomode, and 40 W to splice fiber multimode. In this application microsensor was made with monomode optical fibers. After cleaning carefully with acetone the optical fiber ends, these are installed in parallel in the fusion chamber of the splicer machine, in such a way that the pair of fiber ends is tied and right where the electrical arc will form. This task is not easy the first times, but with a little practice and care, it is routine and effective. Fortunately the system of the splicer has control of axial micropositioning with which the point can be chosen where it is desired to apply the discharge in pair of fiber ends.

2.3 Formation of the semidrop: formation stages

In order to obtain the required optical results with the microsensor, it is very important to obtain the form or model of the semidrop. As all artisan work is necessary to have a serious dominion and knowledge on the operation of the splicer machine, to have absolute control on the final physical form that we wished to give our microsensor. In order to explain the form in which east microsensor of optical fiber was micromachined, we have planned to break down this process into three main steps: fusion of the ends, getting the preform, and obtaining semidrop. These parameters are described in detail, as follows:

2.3.1 Fusion of the ends

Properly placed the fiber ends, as it was explained previously, the discharge of the 20 W electrical arc is practiced automatically, by a lapse of 13 seconds approximately. The place where the electrical arc is due to apply is just, at the end of the pair of ends, as is shown in the Fig. 2.

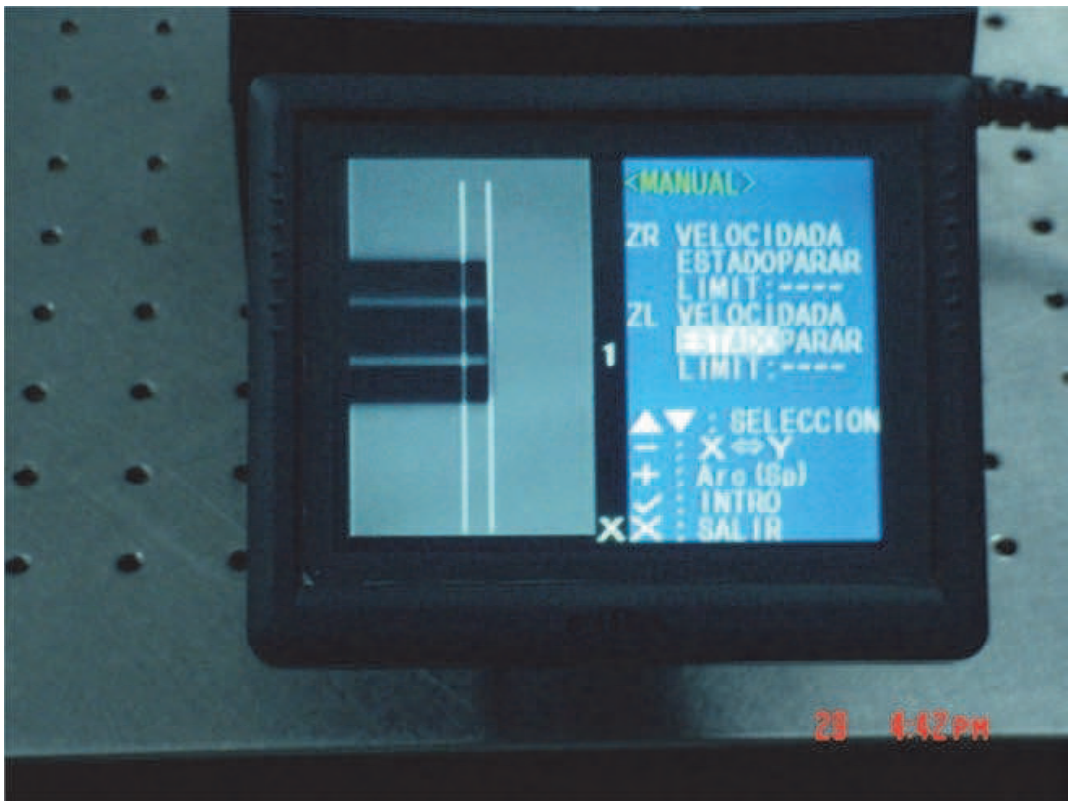


Fig. 2. Application point of the electrical arc (screen on Spanish)

This application has like objective realizing a union that fixes both fiber ends. By means of the application of this electrical arc, the pair of fiber ends reaches the temperature of 1900 °C melt merging and reached a preliminary part of the fiber end with the other, as shown in Fig. 3.



Fig. 3. Fusion of ends

2.3.2 Obtaining of the preform

After the first electrical discharge to have realized, the pair of fiber ends has been fused partially. The following discharging, of the same characteristics, is applied right in the region interface fused fiber-fiber, as it is in the Fig. 4. The objective of this discharging is to approximate the preform obtained towards the physical model of the semidrop.

This is obtained by means of positioning again the pair of fused fibers, just where the discharge will appear, see Fig. 5. 20 W electrical power by 15 seconds is applied after the discharge place has been chosen. Therefore, the following preform of the microsensor has been obtained.

Note physically, the semidrop is already shaped and this stage is called the microsensor preform, see Fig. 6, but is necessary to provide one more a discharging to homogenize, in liquid face, the distribution of refractive indices in the region of the semidrop, to ensure that the microsensor will have a transmittance of not more than 30 dB for the visible or IR region in contact with the air.

2.3.3 Obtaining of the semidrop

The last discharging is applied, just in the curved zone of the preform, as is in the Fig. 7. This discharging also is of the same characteristics, that the previous ones. In this last application,

because the fusion temperature in the region of the semidrop is reached, the splicer machine is due to have in an advisable position to attenuate the effect of the gravity force during the application of the electrical arc, and thus to avoid a deformation in the semidrop geometry. After the electrical discharging applying, Fig. 8, the final conformation microsensor is obtained with the form shown in the Fig. 9. Final dimensions are width 250 μm , and thickness 125 μm .

3. Physical description of the optical fiber microsensor

The optical fiber microsensor is constituted by a pair of parallel optical fibers, where one of the ends of both fibers are joined by controlled electric arc melting, forming a glass semigota, the remaining two fiber terminals work as input and output ends, see Fig. 1. The fibers used are step index, whose core and cladding diameters are respectively 8,3/125 microns, these fibers are commonly used in optical communications, for a wavelength of 1550 nm. The optical fiber microsensor has a transmittance function or transmitted, this function indicates the optical filter response imposed by this microsensor dependent on wavelength, and refractive index of the liquid tested. The optical fibers when transmitting perfectly in the 1550 vicinity nm, do not present attenuation in the region of the microsensor that corresponds to fibers. Nevertheless, the microcavity formed in the fused ends, by its dimensions, geometric, wavelength, and the refractive index of external means, n ; they influence considerably in the behavior of the function of transmittivity of the microsensor. In order to guarantee the same response of the fiber microsensor, the fused ends must describe a glass semidrop.



Fig. 4. Place of application of the electrical arc

In the region of interaction of the semidrop, the microcavity or semidrop constitutes to incident medium (glass), and to medium of transmission it constitutes external means. The reflective properties of the semigota- surrounding medium interface, are regulated by the coefficients of Fresnell, which are not evaluated due to the limitations that impose the dimensions of the microcavity, nevertheless for experimental intentions is advisable to determine the transmittance of the fiber microsensor, $T(\lambda, n)$. This means that if we keep fixed the wavelength of radiation, the transmittance will only be based on the refractive index of surrounding medium, $T(n)$.

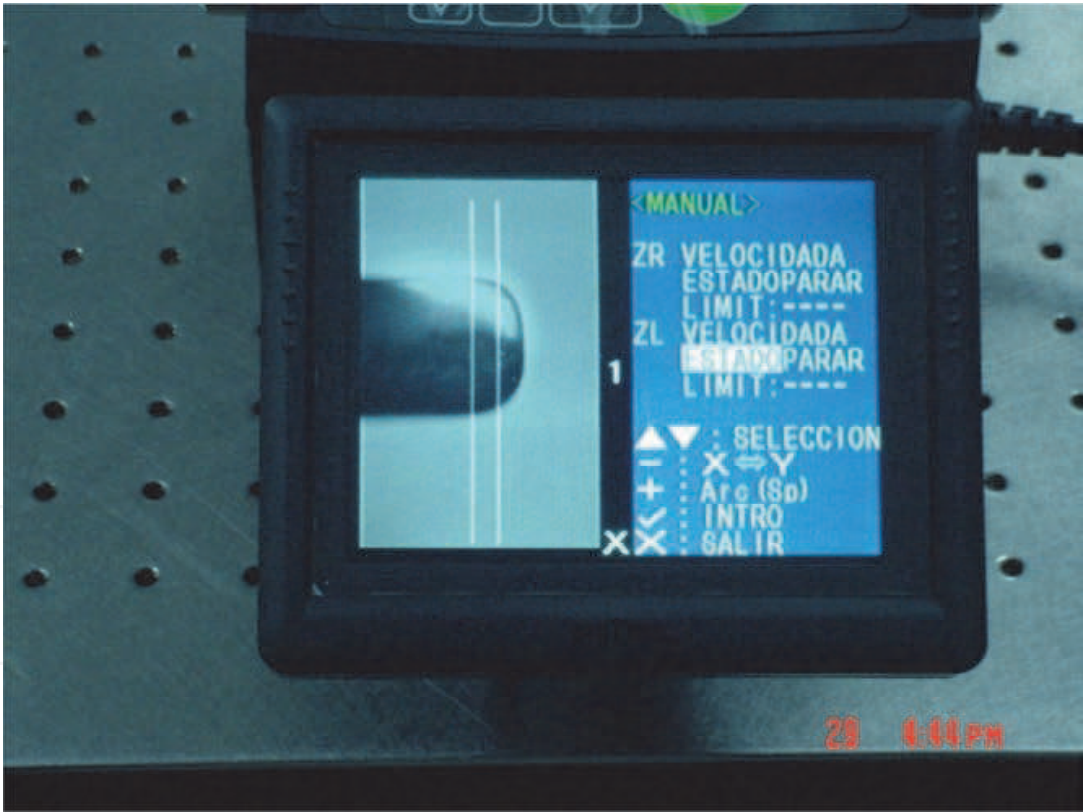
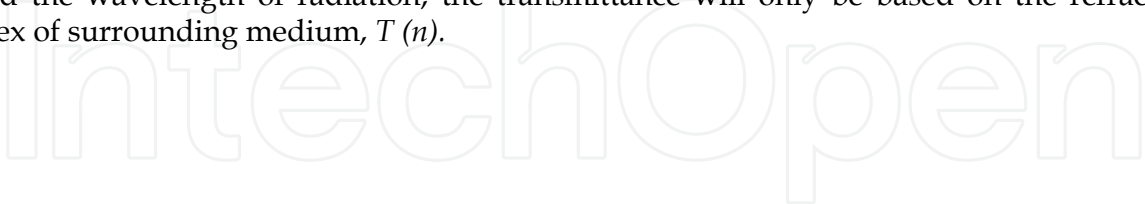


Fig. 5. Application of the electrical arc



Fig. 6. Obtain of the preform



Fig. 7. Place of application of the discharging

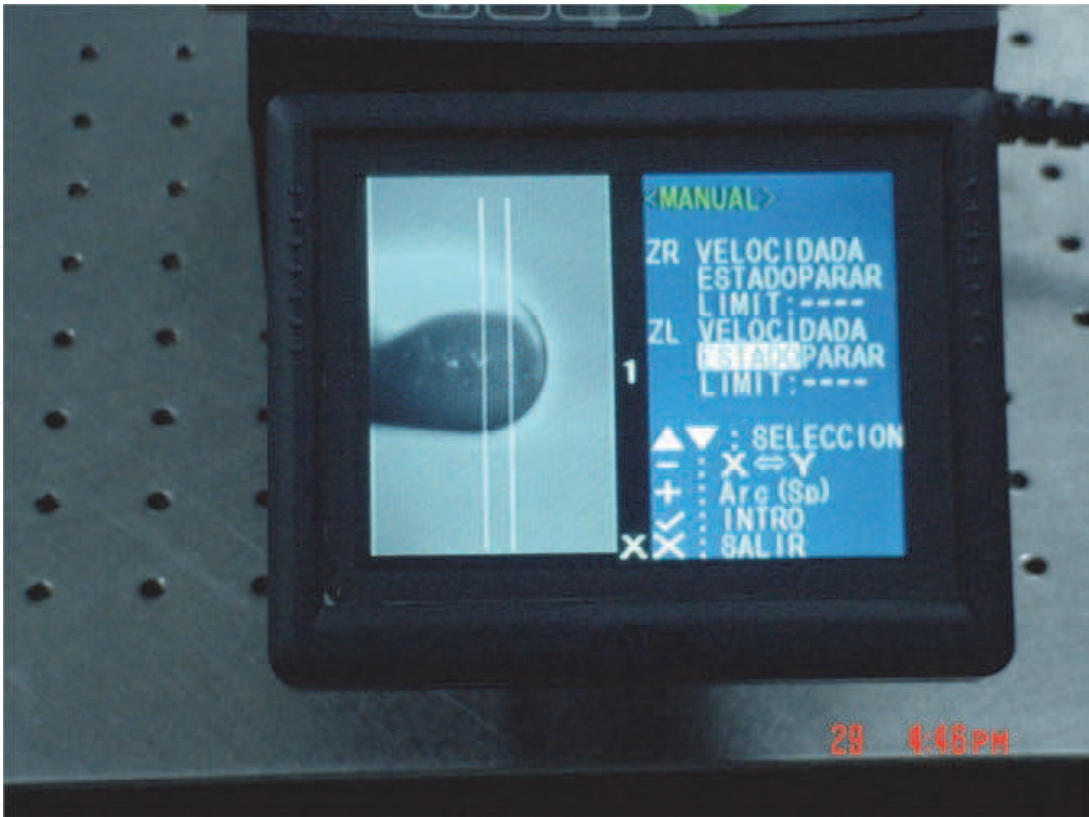


Fig. 8. Application of the electrical arc



Fig. 9. Obtain of the semidrop

4. Theoretical model of the performance of the optical fiber microsensor

The theory of operation of the fiber microsensor starts off of the fact that each pair of immiscible liquids owns its respective refractive indices: n_1 y n_2 . The microsensor of fiber, like optical device, owns its transmittance function that in this case is based on the refractive index of the liquid within which the semidrop of the microsensor is immersed, Eq. 1.

$$T(n) = \frac{P_{out}(n)}{P_{in}} \quad (1)$$

Since the optical power of input, P_{in} , is modified by the reflective properties of the semidrop interface liquid-microsensor in contact, the P_{out} modifies, based on n , of the liquid, and is translated to a V_{pho} of output, by means of a photodetector, that owns a responsivity of voltage, R_v . Eq. (2), illustrates the relation of P_{in} with respect to the measured voltage at the output of the microsensorial system, V_{pho} . A dynamic resistance of the photodetector of 1Ω , is assumed, by simplicity.

$$V_{pho}^2 = R_{volt} P_{out} = R_{volt} T(n) P_{in} \quad (2)$$

Since for each one of the immiscible liquids, including the air, corresponding output voltages, V_{out} . A identification free of errors, offers a high contrast between the associated voltages to each liquid, ΔV , as shown in Eq. 3.

$$\Delta V = V_{phoout2} - V_{phoout1} \quad (3)$$

Considering that the guarantee to operate to the microsensor with two average immiscible liquids, is that the transmittance differences are $\Delta T \neq 0$, implying a nonlinear relation, Eq. 4.

$$0 < \Delta V = \sqrt{R_{volt} \Delta T P_{in}} \quad (4)$$

Sensitivity to both immiscible liquid refractive index, $S(n)$, is described on the basis of which sensitivity in the rapidity of change of output, $T(n)$, with respect to the input n , for the case of our microsensor, Eq. 5.

$$S(\Delta n) = \frac{\Delta T}{\Delta n} \quad (5)$$

where,

$$\frac{\Delta T}{\Delta n} = \frac{T(n_{water}) - T(n_{oil})}{n_{water} - n_{oil}} \quad (6)$$

$$S(\Delta n) = \frac{T(n_2) - T(n_1)}{n_2 - n_1} \quad (7)$$

with respect to the rapidity of commutation of the microsensor, this property rests in the bandwidth of the photodetector used in the microsensorial system. Nevertheless in theoretical terms, the rapidity of commutation, Δt_{rise} , is shown through Eq. 8.

$$\Delta t_{rise} = 0.9(t_2 - t_1) \quad (8)$$

where, t_2 , is the instant where it happens the maximum value, and t_1 , is the instant where the minimum voltage of V_{phoout} happens. Nevertheless in practical terms, and valid for optoelectronic devices, it is possible to be calculated, through Eq. 9.

$$\Delta t_{rise} = \frac{0.35}{BW} \quad (9)$$

where BW is the bandwidth of the photodetector.

5. Experimental results and discussions

Like a pair of immiscible liquids, it has been selected to oil and to the water, by the importance that it has in the economic growth in the world. In this work it was investigated firstly, the effect of the state of polarization of the electric field to the input of the fiber microsensor on the voltage induced in the photodetector, V_{phoout} . The configuration used in this measurement is shown in Fig. 10.

According to Eq. 2, the voltage that appears in the photodetector, V_{phoout} , does not have to depend on the polarization of the incident electric field to the microsensor input. However in the interface semigota-liquid, reflections of Fresnell take place, where the polarization of the incident beams is polarimetrically influenced by the characteristics of the same. In order to verify experimentally, that the voltage that appears in the photodetector, V_{phoout} , is independent of the polarization, it was made vary the state of polarization of the field, \bar{E}_{in} , by means of the use of a polarization controller of three coils.

When varying the angular position of the coil modifies the angular inclination of state of linear polarization of the field, \bar{E}_{in} , to the input of the microsensor. The dependency of the voltage that appears in the photodetector, V_{phoout} , with respect to angle θ , of polarization at the input of the microsensor, as shown in Fig. 11. This experiment was realized at the wavelength of 1550 nm, with interface semidrop-water.

It is appraised that the voltage that appears in the photodetector, V_{phoout} , has small dependency of the angle of polarization. Probably in the region of the semidrop, the dependency of the polarization is remarkable, but this is inhibited by the fiber segments, the input fiber segment, and the output fiber segment, which are standard and non-preservers of the polarization, whose lengths are of not less than 30 cm. In this experiment, the voltage that appears in the photodetector, V_{phoout} , presents fluctuations within the width vicinity $\pm 0,1 \mu V$, which demonstrates that, V_{phoout} , is independent of the polarization.

In order to research the corresponding transmittances for each interaction medium: n_{air} , n_{water} , y n_{oil} , was used an irradiation source that operates in the vicinity of the 1550 nm, for these reason it implemented the gain spectrum of a 10 m segment of erbium doped fiber (EDFA). This irradiation source is an EDFA arrangement without signal at the input, is unidirectional, reason why it emits at the output the spectrum gain of the EDFA, as shown in Fig. 12. EDFA spectrum output is shown in Fig. 13. These spectrums own intensities

different from zero, in the interval from 1500 from 1600 nm. In order to enter this known spectrum at the input of the fiber microsensor, the output of EDFA was coupled with the input end of fiber microsensor

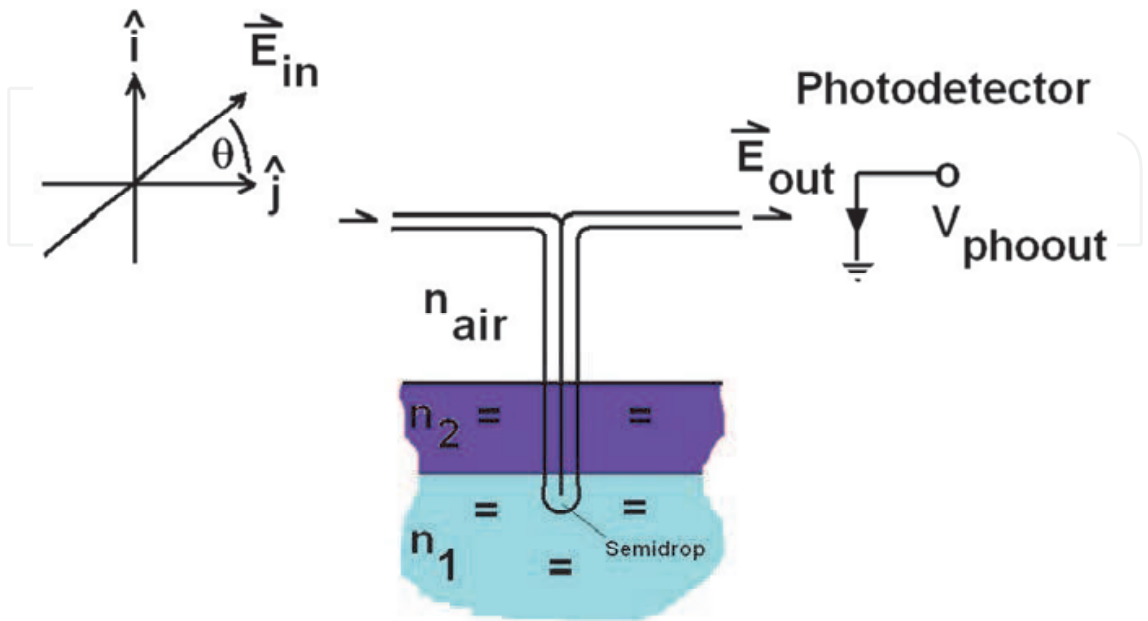


Fig. 10. The semidrop is immersed in two immiscible mediums, whose refractive indices are n_1 , n_2 , additionally n_{air}

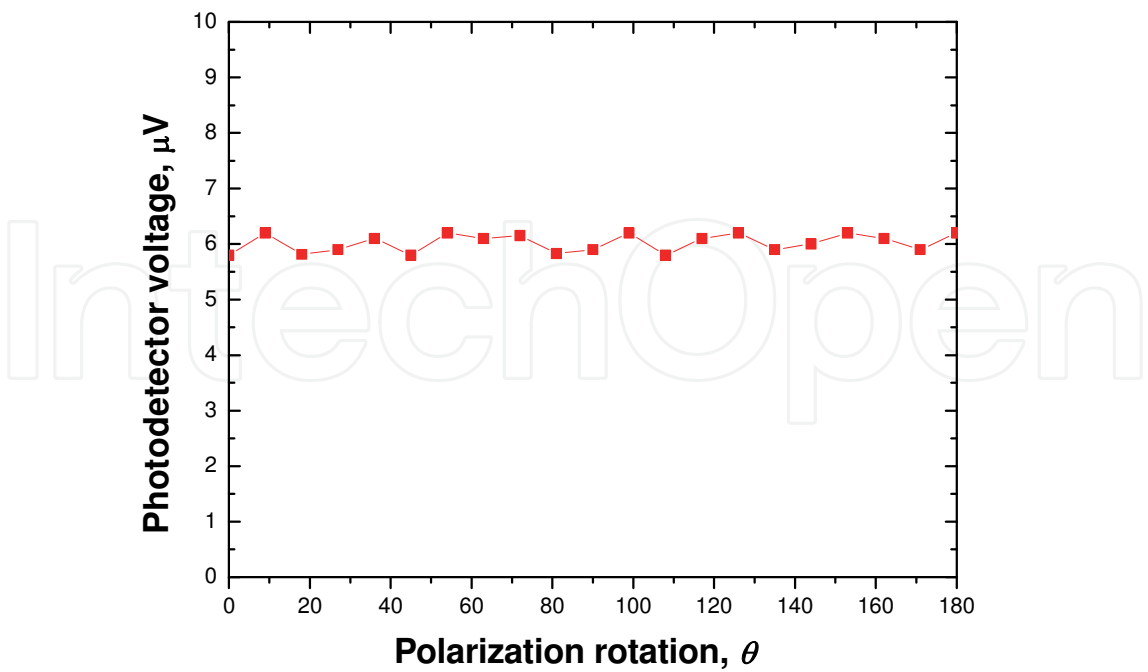


Fig. 11. Voltage variations of the microsensorial system output

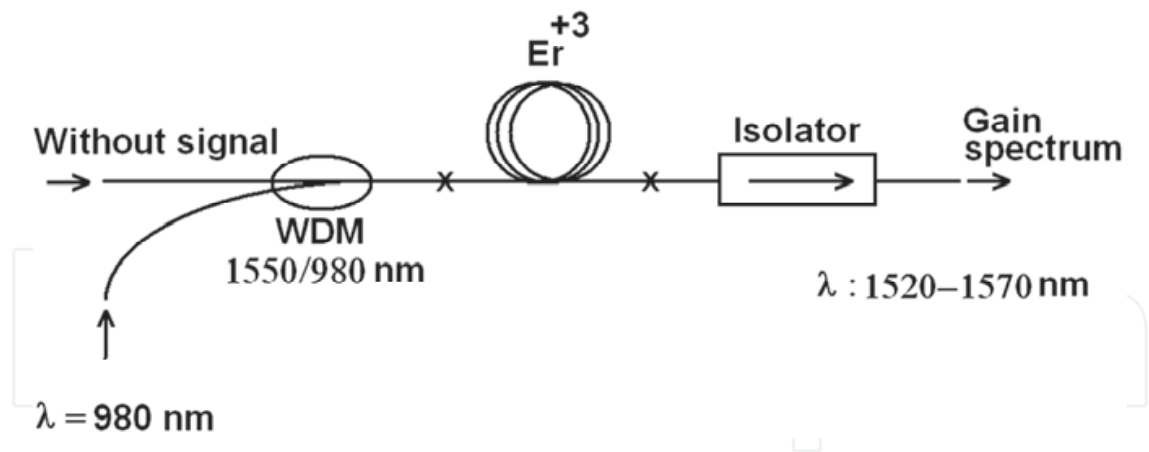


Fig. 12. Setup of EDFA, without input signal

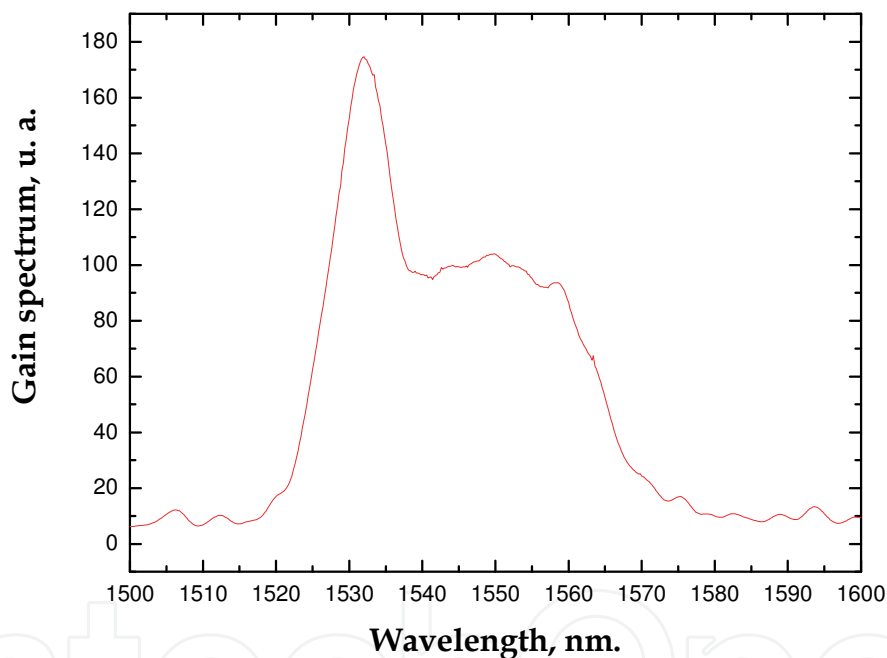


Fig. 13. Irradiation spectrum used to determine the spectral response of optical fiber microsensor

The experimental scheme used to obtain the output spectra is shown in the Fig. 14. The output spectra are useful to determine the functions of transmittance of the microsensor corresponding to each surrounding mediums, according to Eq. 1, for each refractive index n_{air} , n_{water} , and n_{oil} .

The Fig. 15 shows to the value of transmittance functions for each system semigota-water, semidrop-air, and semidrop-oil, in the region of the 1500-1600 nm. These functions are standardized with respect to the transmittance spectrum of the system semidrop-air, which presents the higher peak of transmission in 1527 nm, and it is different from zero from 1508 nm to 1560 nm. The transmittance spectrum of the system semidrop-water presents a peak

in 1522 nm, and it is different from zero from 1515 nm to 1560 nm. The transmittance spectrum of the system semidrop-oil is equal to zero from 1500 nm to the 1600 nm. Reason why to distinguish oil of air, is propitious to use wavelengths in the 1508-1560 nm range, and to distinguish oil of water, is propitious to use wavelengths in the 1515-1560 nm range. Nevertheless, to discriminate the water of oil, the spectral region that offers this possibility, we divided it in two: the one of low contrast, and the one of high contrast. The one of low contrast begins from 1500 to 1515 nm, and from 1534 nm to 1562 nm, as it is possible to be appreciated in the Fig. 15.

The spectral region of high contrast begins from 1523 nm to 1534 nm. This procedure ensures the success of operation of the optical fiber microsensor, and it is attainable for any other pair of immiscible liquids of industrial or biomedical interest.

Remarkable contrast exists in the values of $T(n)$ for the mediums air, oil and air for the wavelength of 1550 nm, as is shown in Fig. 16. During the experiment and measuring, the decays of power, P_{out} , were measured in percentage of the power compared with the output power. In other words, the P_{out} of the system semigota-air represents the 100% of the microsensor.

When submerging the microsensor towards oil, was observed a reduction to 0,0% of the la P_{out} power of the air. Nevertheless, when the microsensor made contact with the water, the power was restituted to 18,5% with respect to the P_{out} of the air. These results are in Table 1. These data show the capacity of discrimination of the microsensor for the wavelength of 1550 nm.

In order to demonstrate the effectiveness of microsensor of fiber for the detection of the interfaces formed by immiscible liquids, the graph shown in the Fig. 17 was developed. In this graph the changes of transmittance acquire knowledge that detects the microsensor of fiber, when realizing an orthogonal sweeping, from the bottom towards the surface, crossing the interfaces that form in a tank cistern that contains interfaces water-oil, h_{water} , oil-air, h_{oil} .

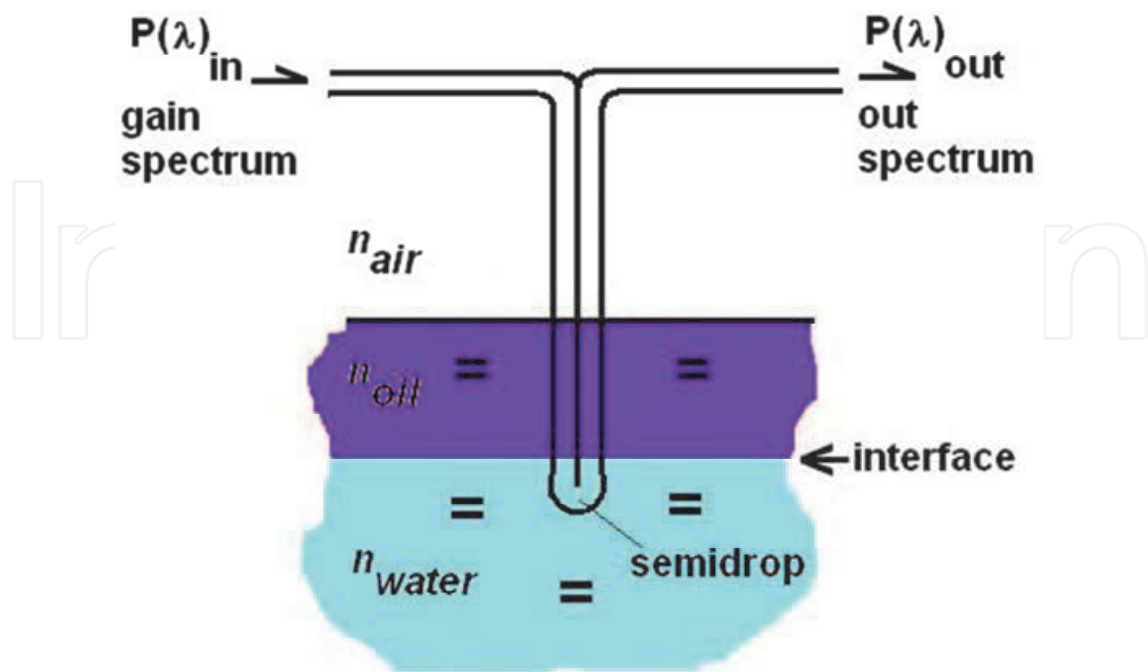


Fig. 14. Experimental setup to obtain output spectrum in the IR region (1550-1600nm)

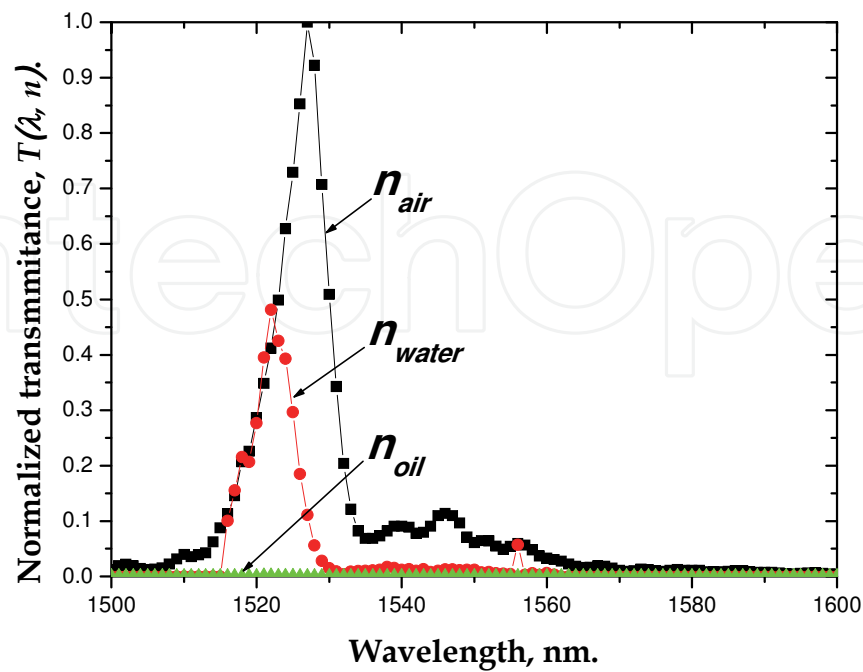


Fig. 15. Transmittance spectra for semigota-water systems, semigota-air, and semigota-oil

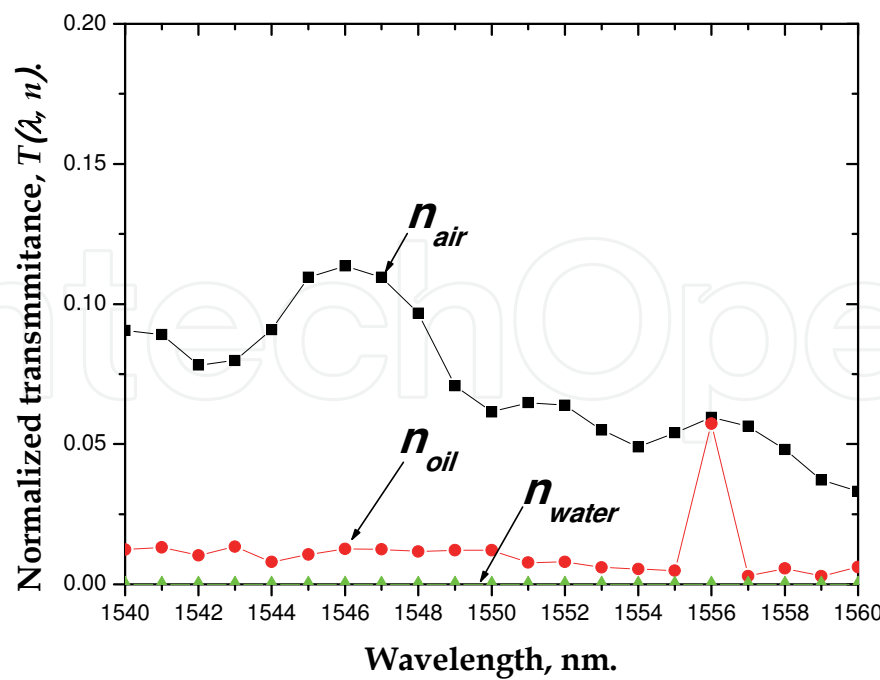


Fig. 16. Spectral region of low contrast to n_{water} and n_{pil} detection

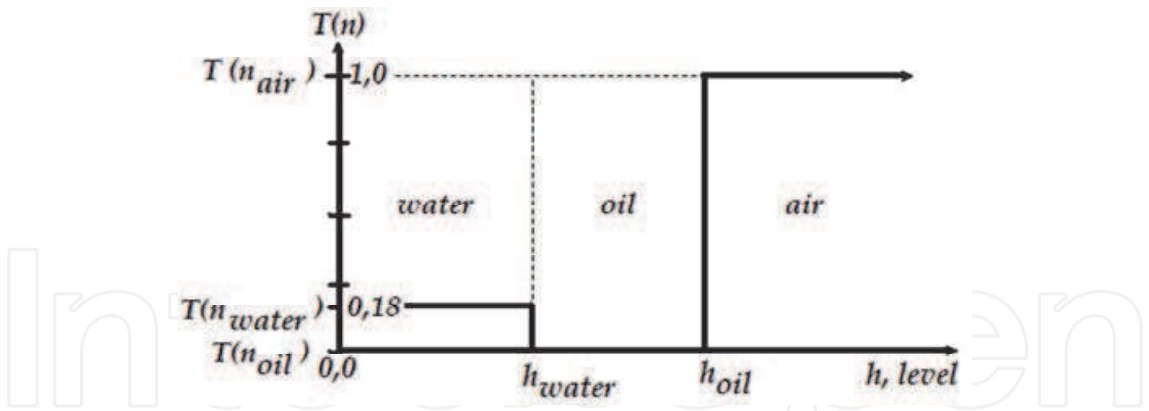


Fig. 17. Transmittance values corresponding to levels of water, oil, and air

It is observed that in these levels, a commutation in the transmittance of the fiber microsensor happens, that is interpreted like the existence of each of these interfaces that appear in the axis of h , level. This evaluation was performed for a wavelength of 1550 nm. Note that the maximum transmittance for semidrop-air system, considered as 100% for the semidrop-water system is 18,5%, and semidrop-oil system is zero. For this reason, the fiber microsensor is functional for the detection of interfaces formed between the two immiscible liquids.

To research the sensitivity of the optical fiber microsensor, referred to Eq. 7, which requires the information specified in Table 1, and the indices of refraction of water 1,3, oil 1,48, and air 1,0. Note in Table 2, the fiber microsensor has a high sensitivity to cross the air-oil, because the change of transmittance is from 1,0 to 0,0, for a small variation of refractive indices. In the case of oil-water interface, transmittance values are very close, as their refractive indices, so that the sensitivity of fiber microsensor suffers a significant reduction.

Surrounding medium	$T(n)$ to 1550 nm, (%)
air	100
water	18,5
oil	0,0

Table 1. Percentage decay of the microsensor $T(n)$

Interfaces	$S(\Delta n)$
water-oil	1,0
oil-air	2,0

Table 2. Optical fiber microsensor sensitivity

With a similar procedure and by using a white radiation source (light emitting diode of high brightness) and a silicon photodetector, gives the percentage values of $T(n)$ of the system interacting with the same mediums, see Table 3. Note that the contrast in the detection for the air, water and oil has improved. The advantage to radiate with white light source is that, all wavelengths of the interval from 390 to 780 nm have contributed, so photodetector collect more power.

<i>Surrounding medium</i>	<i>T(n) to 390-780 nm, (%)</i>
air	100
water	13
oil	20

Table 3. Percentage decay of the microsensor $T(n)$ for visible region

Like any proximity sensor device, the optical fiber microsensor when passing the interface of air, oil, and water, indirectly reports the location of the interface, by location or area of switching their output voltages: H (high) or L (low). Knowledge of minimum time, that the microsensor can resolve a change of medium, is of importance to the location of the interfaces of immiscible liquids. The switching speed of the microsensor is strongly restricted by the bandwidth of the photodetector to the optical output of the microsensor (13 kHz). Under this, to know the response time of the microsensor, it applies the criterion of rise time, t_r , (risetime) with respect to bandwidth of LTI system, which in this case is the bandwidth, BW, of InGaAs photodetector. The relationship applied in this deduction is for Eq. 9, so that, $t_r = 26,92 \mu m$. Finally, the finish of fiber optic microsensor is shown in Fig. 18, and specifications of optimized optical fiber microsensor are shown in Table 4.

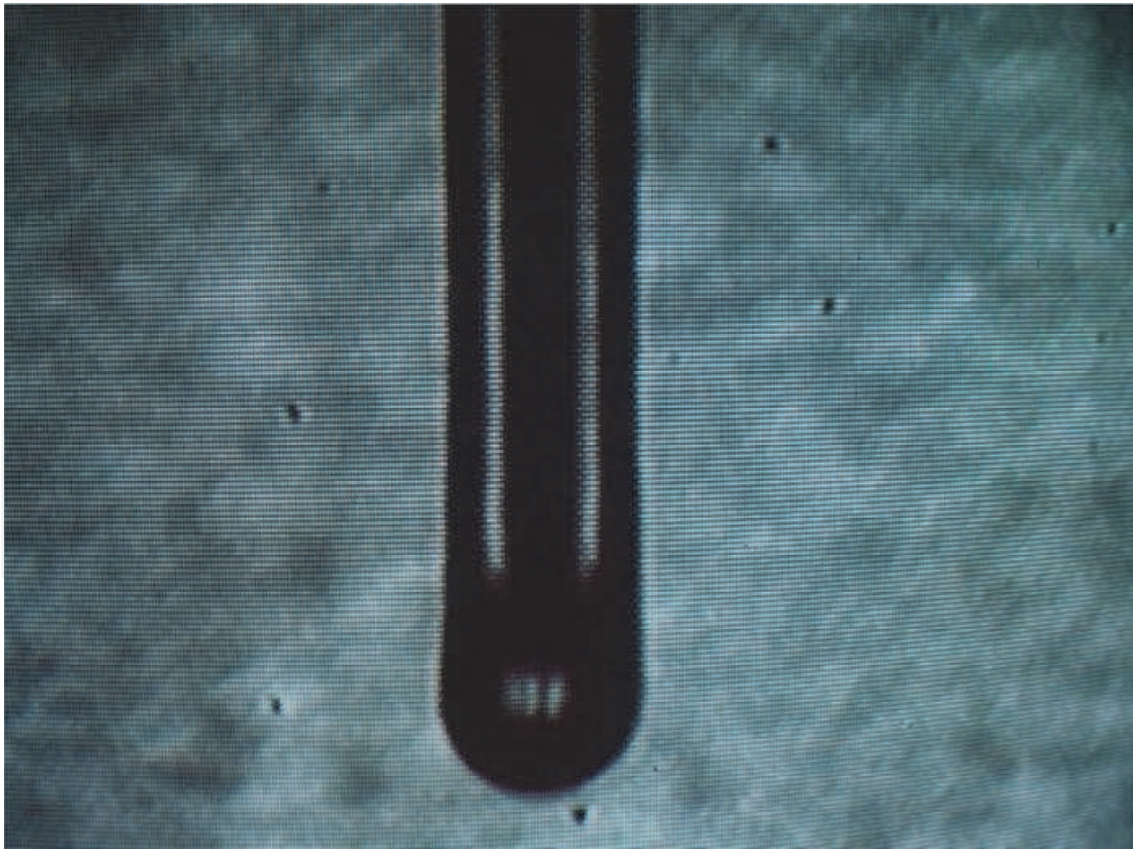


Fig. 18. Physical illustration of the optical fiber microsensor, increased 220 times in a monitor screen

<i>Elements</i>	<i>Characteristics</i>
Optical fibers	8,3/125 μm
ILD	$1550 \pm 0,5 \text{ nm}$
Power range	5 mW - 6,5 mW
Photodetector	Si low power, BW= 1,75 MHz
Max. response time	$< 2 \mu\text{s}$
Dynamic range	Refractive index $< 1,9$
Sensitivity	$- 5,714 \times 10^{-4} \mu\text{V}$, water-oil
Temperature	$0^\circ \text{ a } 50^\circ \text{C}$

Table 4. Specifications of optimized optical fiber microsensor

6. Conclusions

This research has shown that the fiber optical microsensor is possible to manufacture by electric arc technology. We demonstrated that is possible to improve the response detection of optical fiber microsensor, for certain immiscible liquids, by proper choice of a specific wavelength. This wavelength or radiation spectral region should provide a high discrimination of the two liquids. Speed detection of the microsensor, strongly dependent on the bandwidth of the photodetector. The method used in this research can be applied in the detection of other mediums, including other regions of the optical spectrum. Due to geometrical and physical properties of fiber microsensor, it can be applied to biomedicine, because it is micrometer-scale, flexible like being guided in an artery or a catheter inserted, and it is easy to sterilize. As future research work, we have considered using the microsensor to implement a system of characterization and recognition of organic and inorganic liquids (alcohols, acids, neutrals, blood, urine, water, etc.) by using spectroscopy in the infrared and/or visible region. Optical fiber microsensor represents an alternative in the industrial applications, and mainly in the detection of explosive, corrosive and/or highly harmful liquids, for the human being.

7. Acknowledgment

We are thankful to the Benemérita Universidad Autónoma de Puebla, and the group of full professors of the Facultad de Ciencias de la Electrónica, Optoelectronic department, by to have looked for at the time, the ways and possibilities, to acquire these efficient equipments of measurement, to have been able to make reality this project.

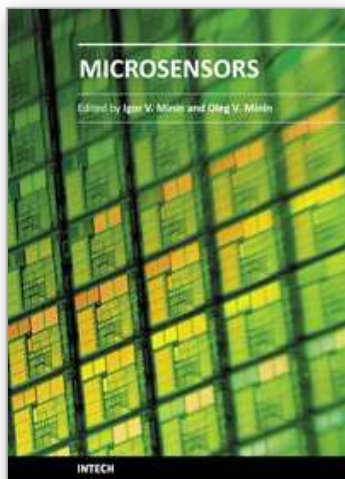
8. References

De Leon , V. & Khotiaintsev, S. (1996). Raytracing in the design of microoptical sensors used for the determination of refractive index of surrounding media. *Proceeding of SPIE, Infrared Spaceborne Remote Sensing IV* ,Vol. 2817, pp. 299-311, ISBN 9780819422057, Denver, CO, USA, 1996

Jones, O. C. & Zimmer, G. A. (1978). Optical probe for local void fraction and interface velocity measurements, *Review of Scientific Instruments*, Vol. 49, No. 8, (August 1978), pp. 1090-1094, ISSN 0034-6748

- Molina-Flores, E. et al, (1995). Fiber-optic multipoint high-resolution level-sensor for biomedical applications. *Proceeding of SPIE, Medical and Fiber Optic Sensors and Delivery Systems*, Vol. 2631, pp. 121-126, ISBN 9780819419958, Barcelona, Spain, 1995
- Molina-Flores, E., Aguilar-Jiménez, O. & Molina-Flores, D. (2006). Microsensor refractométrico discreto de fibra óptica para detección de interfaces petróleo-agua, operando en la región visible. *Internet Electrón. J. Nanocs. Moletrón*, Vol. 4, No. 3, (December 2006), pp. 815-826, ISSN 0188-6150
- Svirid, V.; Khotiaintsev, S. & Swart, P. L. (2002). Novel optical fiber refractometric transducer employing hemispherical detection element, *Optical Engineering*, Vol. 41, No. 4, pp. 779-787, ISSN 0091-3286
- Volodymyr, S., & Khotiaintsev, S., (2000). Optoelectronic multipoint liquid level sensor for light petrochemical products, *Proceedings of SPIE, Optoelectronic and Hybrid Optical/Digital Systems for Image and Signal*, Vol. 4148, pp. 262-268, ISBN: 9780819437952, 2000

IntechOpen



Microsensors

Edited by Prof. Igor Minin

ISBN 978-953-307-170-1

Hard cover, 294 pages

Publisher InTech

Published online 09, June, 2011

Published in print edition June, 2011

This book is planned to publish with an objective to provide a state-of-art reference book in the area of microsensors for engineers, scientists, applied physicists and post-graduate students. Also the aim of the book is the continuous and timely dissemination of new and innovative research and developments in microsensors. This reference book is a collection of 13 chapters characterized in 4 parts: magnetic sensors, chemical, optical microsensors and applications. This book provides an overview of resonant magnetic field microsensors based on MEMS, optical microsensors, the main design and fabrication problems of miniature sensors of physical, chemical and biochemical microsensors, chemical microsensors with ordered nanostructures, surface-enhanced Raman scattering microsensors based on hybrid nanoparticles, etc. Several interesting applications area are also discusses in the book like MEMS gyroscopes for consumer and industrial applications, microsensors for non invasive imaging in experimental biology, a heat flux microsensor for direct measurements in plasma surface interactions and so on.

How to reference

In order to correctly reference this scholarly work, feel free to copy and paste the following:

Esteban Molina-Flores, R. B. López-Flores, Daniel Molina-Flores, José A. Dávila-Píntle, Germán A. Muñoz-Hernández Carlos A. Gracios-Marín and Enrique Morales-Rodríguez (2011). Optical Fiber Microsensor of Semidrop, Microsensors, Prof. Igor Minin (Ed.), ISBN: 978-953-307-170-1, InTech, Available from: <http://www.intechopen.com/books/microsensors/optical-fiber-microsensor-of-semidrop>

INTECH
open science | open minds

InTech Europe

University Campus STeP Ri
Slavka Krautzeka 83/A
51000 Rijeka, Croatia
Phone: +385 (51) 770 447
Fax: +385 (51) 686 166
www.intechopen.com

InTech China

Unit 405, Office Block, Hotel Equatorial Shanghai
No.65, Yan An Road (West), Shanghai, 200040, China
中国上海市延安西路65号上海国际贵都大饭店办公楼405单元
Phone: +86-21-62489820
Fax: +86-21-62489821

© 2011 The Author(s). Licensee IntechOpen. This chapter is distributed under the terms of the [Creative Commons Attribution-NonCommercial-ShareAlike-3.0 License](https://creativecommons.org/licenses/by-nc-sa/3.0/), which permits use, distribution and reproduction for non-commercial purposes, provided the original is properly cited and derivative works building on this content are distributed under the same license.

IntechOpen

IntechOpen